nature photonics

ARTICLES

https://doi.org/10.1038/s41566-018-0156-x

Enrichment of molecular antenna triplets amplifies upconverting nanoparticle emission

David J. Garfield[1,2,8], Nicholas J. Borys[1,8], Samia M. Hamed[2], Nicole A. Torquato[1], Cheryl A. Tajon[1], Bining Tian[1], Brian Shevitski[1,3], Edward S. Barnard[1], Yung Doug Suh[4,5], Shaul Aloni[1], Jeffrey B. Neaton[1,3,6], Emory M. Chan[1*], Bruce E. Cohen[1*] and P. James Schuck[1,7*]

Efficient photon upconversion at low light intensities promises major advances in technologies spanning solar energy harvesting to deep-tissue biophotonics. Here, we discover the critical mechanisms that enable near-infrared dye antennas to significantly enhance performance in lanthanide-doped upconverting nanoparticle (UCNP) systems, and leverage these findings to design dye–UCNP hybrids with a 33,000-fold increase in brightness and a 100-fold increase in efficiency over bare UCNPs. We show that increasing the lanthanide content in the UCNPs shifts the primary energy donor from the dye singlet to its triplet, and the resultant triplet states then mediate energy transfer into the nanocrystals. Time-gated phosphorescence, density functional theory, singlet lifetimes and triplet-quenching experiments support these findings. This interplay between the excited-state populations in organic antennas and the composition of UCNPs presents new design rules that overcome the limitations of previous upconverting materials, enabling performances now relevant for photovoltaics, biophotonics and infrared detection.

Photon upconversion, the process of combining multiple low-energy photons into a single higher-energy photon, underlies advanced optical technologies in solar light harvesting[1–3], deep-tissue bioimaging[4,5], sensing[6] and optogenetics[7,8]. Two multiphoton techniques, molecular triplet–triplet annihilation[9–11] (TTA) and multistep absorption in lanthanide-doped upconverting nanoparticles (UCNPs) show exceptionally efficient anti-Stokes emission and each have specific advantages depending on the wavelengths, fluences and desired applications. The current study focuses on UCNP systems, which are capable of upconverting near-infrared (NIR) light five to six orders of magnitude more efficiently than other nonlinear optical materials[2]. Consisting of an optically inert ceramic matrix doped with photoactive lanthanide ions such as Yb^{3+} and Er^{3+}, UCNPs take advantage of the long-lived intermediate energy states within the lanthanide ions[12] to sequentially absorb multiple photons at low excitation intensities, enabling efficient anti-Stokes emission[2,4,13,14]. Recent studies have shown that attachment of organic dye antennas to UCNP surfaces dramatically increases their optical cross-sections and absorption bandwidths[1,7,15–18], potentially transforming a range of fields. However, existing studies demonstrate either large emission enhancement[1] or increased upconverting efficiencies[7,15–17] when dye antennas are attached to the UCNPs, but not both. This highlights a lack of general understanding surrounding the dye–nanocrystal interactions, which currently prevents their use in any practical applications.

In this Article, we reveal that spin-triplet states in the dye antennas act as key intermediates in the sensitization of the UCNPs, and, further, that lanthanide ions at the UCNP surface enhance intersystem crossing (ISC) within the dye from the singlet (S_1) to triplet (T_1) excited states through the heavy atom effect, where ISC $\propto Z_{\text{eff}}^4$ (Fig. 1; Z_{eff}, effective nuclear charge)[19]. Leveraging the importance of dye triplet states and the influence that UCNP composition holds on their population, we produce sub-20 nm nanoparticles with upconverted emission more than four orders of magnitude brighter than that of non-sensitized UCNPs.

Evidence of a resonant triplet

We chose to investigate the means of energy transfer from the cyanine dye antenna IR806[1,7,15,18], which is commonly coupled to UCNPs despite the weak spectral overlap of its fluorescence with the absorption of the UCNP Yb^{3+} sensitizer (Supplementary Methods and Supplementary Fig. 1)[1,15]. We used time-gated photoluminescence spectroscopy to search for a relatively dark lower-energy phosphorescent state of the dye that better overlaps with Yb^{3+} absorption, potentially explaining efficient energy transfer (Supplementary Methods and Supplementary Fig. 2). Thin films of IR806 in polystyrene cooled to 80 K yielded no detectable delayed luminescence. Recognizing that ISC to the triplet state could be enhanced by proximal lanthanides in the UCNPs[20–23], we attached IR806 dyes to optically inert $NaGdF_4$ nanoparticles (that is, without Yb^{3+} or Er^{3+}), a common host matrix for UCNPs with luminescent transitions only in the ultraviolet[24]. Following excitation at 791 nm, films of IR806–$NaGdF_4$ nanoparticles in polystyrene exhibit a long-lived peak centred at 981 nm, close to the 976 nm absorption maximum of the sensitizing Yb^{3+} transition ${}^2F_{7/2} \rightarrow {}^2F_{5/2}$ (Fig. 2a). This spectrum was taken with a 10 μs delay relative to singlet emission ($\tau_{\text{singlet}} = 575$ ps), ensuring that the signal originates from long-lived phosphorescence. Excitation spectroscopy confirmed the presence of a lower energy state at 980 nm (Supplementary Figs. 3 and 4). To confirm the origins of these emissions, we used time-dependent density functional theory (TD-DFT) within the Tamm–Dancoff approximation (TDA) and standard global and range-separated hybrid exchange-correlation

---

[1]The Molecular Foundry, Lawrence Berkeley National Laboratory, Berkeley, CA, USA. [2]Department of Chemistry, University of California, Berkeley, CA, USA. [3]Department of Physics, University of California, Berkeley, CA, USA. [4]Research Center for Convergence NanoRaman Technology, Korea Research Institute of Chemical Technology, DaeJeon, South Korea. [5]School of Chemical Engineering, Sung Kyun Kwan University (SKKU), Suwon, Korea. [6]Kavli Energy NanoSciences Institute at Berkeley, Berkeley, CA, USA. [7]Department of Mechanical Engineering, Columbia University, New York, NY, USA. [8]These authors contributed equally: David J. Garfield, Nicholas J. Borys. *e-mail: emchan@lbl.gov; becohen@lbl.gov; p.j.schuck@columbia.edu

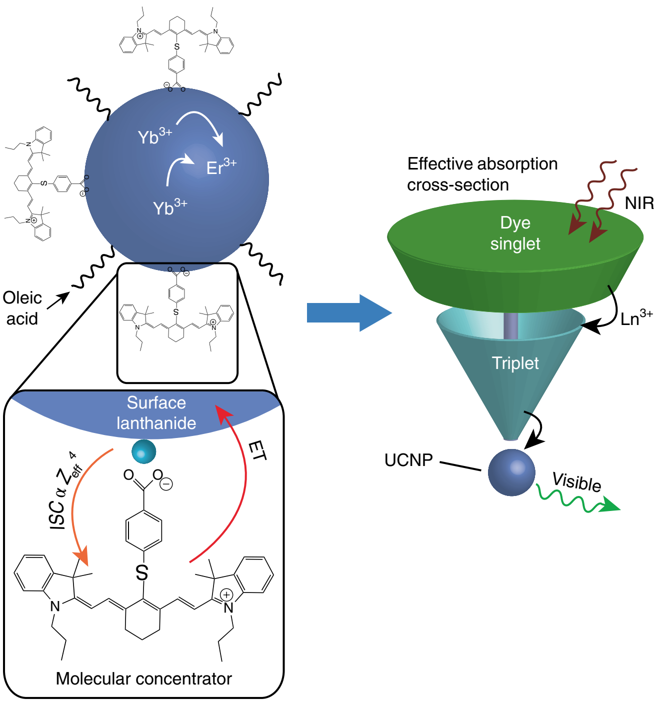

Fig. 1 | Dye-functionalized UCNPs, their mechanism of energy transfer, and the larger effective absorption cross-section of dyes relative to UCNPs. Top left, Cartoon schematic of the dye-sensitized UCNP system, showing IR806 bound to the UCNP surface (not to scale), and an upconversion event inside the UCNP where two excited Yb^{3+} non-radiatively and sequentially excite an Er^{3+} into a higher energetic state. Bottom left, Magnified illustration of the interactions between IR806 and a surface lanthanide—the heavy nucleus of the lanthanide aids in ISC from IR806 $S_1 \rightarrow T_1$ states, allowing much more efficient T_1 sensitization of the Ln^{3+} atoms within the UCNP. Right, Depiction of the antenna-like nature of IR806 in sensitizing the UCNP upconversion, conveying the much larger absorption cross-section of IR806 relative to the UCNP, as well as $S_1 \rightarrow T_1$ ISC enhancement by Ln^{3+}.

functionals to calculate vertical excitation energies for the T_1 state of IR806 in the range 0.9–1.2 eV, in close agreement with the experimentally determined value (Fig. 2b, Supplementary Table 1, Supplementary Methods). Interestingly, the ground-state molecular configuration of IR806 suggests that the sulfur bridge may facilitate triplet energy transfer, bringing the frontier π orbital to within ~3–7 Å of the nanoparticle surface. The relevant transitions and energy transfer pathways in the dye-sensitized UCNP system (Fig. 2c,d) highlight the weak spectral overlap of the dye S_1 state with absorbing UCNP lanthanides and the direct overlap of the T_1 state with the Yb^{3+} and Er^{3+} absorption spectra (Supplementary Methods).

Enhancing triplet populations

Based on this new understanding of the IR806 triplet manifold, we sought to modify the UCNP composition to rationally enhance the dye triplet population. Although triplet states have been shown to donate energy to nanoparticles and, separately, to accept energy from nanoparticles[25–30], the concept of altering nanoparticle composition to increase the number of dye triplets, which in turn enhance energy transfer to and emission from the nanoparticle, has not been described (Fig. 1). We varied the heavy atom content by adjusting the ratio of Y^{3+} to Gd^{3+} ions, synthesizing ~12 nm UCNPs with either 0 or 30% Gd^{3+} (β–NaY$_{0.78-x}$Gd$_x$Yb$_{0.2}$Er$_{0.02}$F$_4$), and functionalized these with IR806, prepared and sealed without water or O$_2$ (Supplementary Figs. 5–10 and Supplementary Methods). Neither Gd^{3+} nor Y^{3+} have optical transitions in the NIR or visible and thus do not directly participate in the photophysical transitions that give rise to NIR-to-visible upconversion[31]. For UCNPs with 0% Gd^{3+}, dye sensitization ($\lambda_{\mathrm{ex}} = 808$ nm) enhances the upconverted emission intensity ~500-fold over direct UCNP excitation ($\lambda_{\mathrm{ex}} = 980$ nm) using the same excitation power density at both wavelengths (1×10^3 W cm^{-2}), an enhancement similar to previous reports[1]. Dye sensitization of the 30% Gd^{3+} UCNPs, however, enhances upconverted emission intensity ~15,000-fold over direct UCNP excitation at the same excitation density. Thus by raising the Gd^{3+}content, we increase the spin–orbit coupling and ISC kinetics within the dye by increasing the average Z_{eff} of atoms on the UCNP surface[20–23], yielding an additional 30-fold enhancement in upconverted emission (Fig. 3a). These spectra were taken with 5 W cm^{-2} excitation power density, highlighting the potency of using light antennas to lower the required excitation flux. Signal-to-noise analysis (Supplementary Methods) of Fig. 3a further shows that fluences less than 100 mW cm^{-2} can give a measurable signal. This result demonstrates that, in dye-sensitized UCNPs, the lanthanide composition may be optimized concurrently with dye sensitization to achieve maximum performance, due to the coupled nature of these systems.

Quantification of triplet energy sensitization of UCNPs

To determine the extent to which UCNP lanthanide content influences IR806 photophysics, we measured singlet relaxation dynamics in the presence and absence of UCNPs (Fig. 3b). Free IR806 in solution has a characteristic singlet lifetime, τ_{F}, of 575 ps, yet bound to the surface of 0% Gd^{3+} UCNPs, it shortens by about half to 293 ps. This is indicative of Förster resonance energy transfer (FRET) from the dye singlet to Yb^{3+}, although with 22% Ln^{3+} content, we believe a small amount of this decay is caused by ISC to the dye triplet state, which is supported by the triplet quencher experiments described in the following paragraph (Fig. 3c). When bound to the surface of 30% Gd^{3+} UCNPs, the IR806 singlet lifetime shortens even more to 173 ps. Because the Yb^{3+} and Er^{3+} contents remain constant, the FRET rate from the dye is not expected to change, and therefore this shortening of the singlet lifetime can be entirely attributed to an increase in ISC, suggesting the dye is not only close enough to the UCNP lanthanides for FRET, but close enough to be influenced by the heavy atom effect[19–23] of the UCNP Gd^{3+} nuclei. The increased heavy atom effect then increases ISC within the dye approximately eightfold, resulting in the shortened lifetime of 173 ps. We also note the absence of an unquenched component in the fluorescence transients of the IR806–UCNP complexes, suggesting that free IR806 contributes little to the measured emission.

To further quantify the energy transfer contribution of these triplets into the UCNPs, and to verify that the triplet acts as an intermediate in sensitizing upconversion within the UCNPs, we sought to systematically quench energy transfer from the triplet manifold of the dye. The triplet quencher cyclooctatetraene (COT) was used as a molecule known to selectively scavenge excited-state triplets in organic dyes because of its high-energy singlet state (4.39 eV) and low-lying triplet state (0.8 eV)[32–34], enabling COT to quench triplets without siphoning excited-state singlets. The upconverted quantum yield (UCQY) of dye-sensitized UCNPs was measured in the presence of increasing amounts of COT, and while UCNPs with 0% Gd^{3+} showed a decrease of UCQY by ~25%, UCNPs with 30% Gd^{3+} content showed a decrease of UCQY by ~65% (Fig. 3c). This not only provides compelling evidence that significant energy transfer to the UCNP occurs via molecular antenna triplets, but that lanthanide content within the UCNP influences ISC rates and thereby triplet populations.

These long-lived triplets are known to suffer from photooxidation by ambient water and reactive oxygen species[35], presenting a challenge for using dye–UCNP complexes. Changes in the steady-state absorption of dyes bound to UCNPs suggest that they are

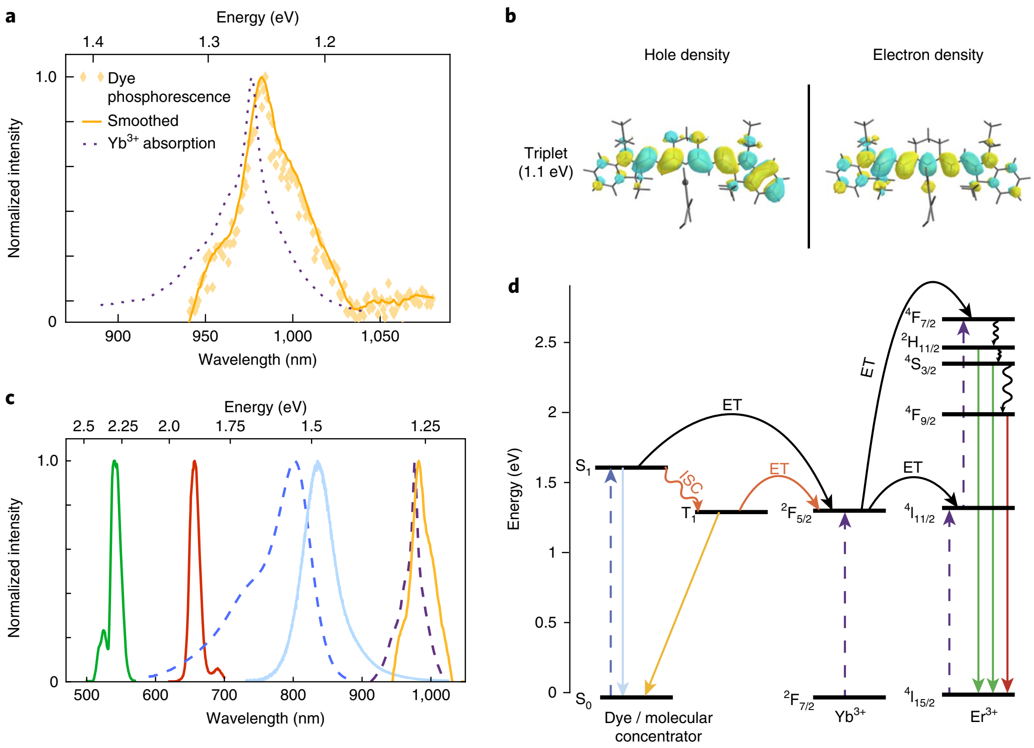

Fig. 2 | Time-gated photoluminescence as evidence of resonant triplet states. **a**, Time-gated triplet phosphorescence spectrum of IR806 on $NaGdF_4$ nanoparticles at 80 K (no Yb^{3+} or Er^{3+} present), overlaid with the NIR portion of the UCNP absorption spectrum (at room temperature). **b**, Electronic densities of the natural transition orbital (NTO) of the hole and the NTO of the electron for the first excited triplet state of IR806, calculated using TD-DFT with the TDA and the B3LYP functional. **c**, Spectra from left to right, coloured according to their transitions in **d**: Er^{3+} emission (green and red curves), IR806 absorption (dashed blue curve), IR806 fluorescence (solid, light blue curve), UCNP absorption (dashed purple curve) and IR806 phosphorescence (yellow curve). **d**, Jablonksi diagram of proposed energy transfer (ET) landscape, showing dye ISC to the triplet state T_1 before transfer to UCNP lanthanides.

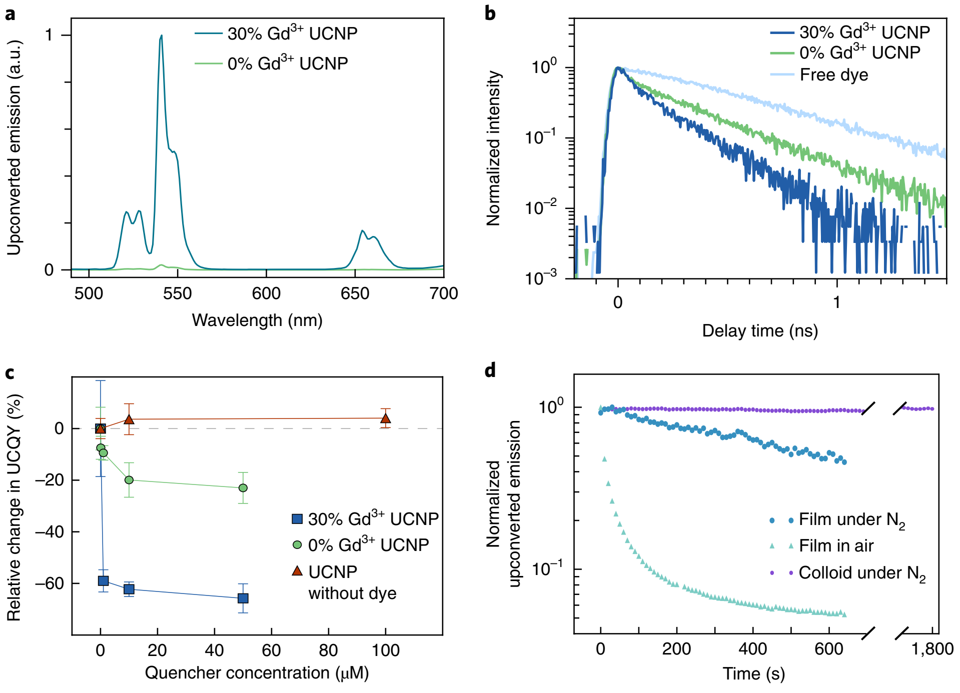

Fig. 3 | Evidence of triplet energy transfer to UCNPs. **a**, Upconverted emission from dye-sensitized UCNPs with 30% Gd^{+3} (blue line) and with 0% Gd^{3+} (green line). Excitation power, ~5 W cm^{-2}. **b**, IR806 singlet emission lifetimes for free dye (top curve, $\tau = 575$ ps), bound to 0% Gd^{3+} UCNPs (middle curve, $\tau = 293$ ps), and bound to 30% Gd^{3+} UCNPs (bottom curve, $\tau = 173$ ps). **c**, Relative change in upconverted quantum yield (UCQY) of 30% Gd^{3+} (blue squares) and 0% Gd^{3+} IR806–UCNPs (green circles), as well as UCNPs without dye (orange triangles) as a function of the concentration of the triplet quencher cyclooctatetraene. Error bars represent one standard deviation from the mean. **d**, Temporal photodegradation of upconversion from 30% Gd^{3+} IR806–UCNP films in air (light blue) or encapsulated under N_2 (dark blue), as well as a colloidal suspension in toluene under N_2 (purple).

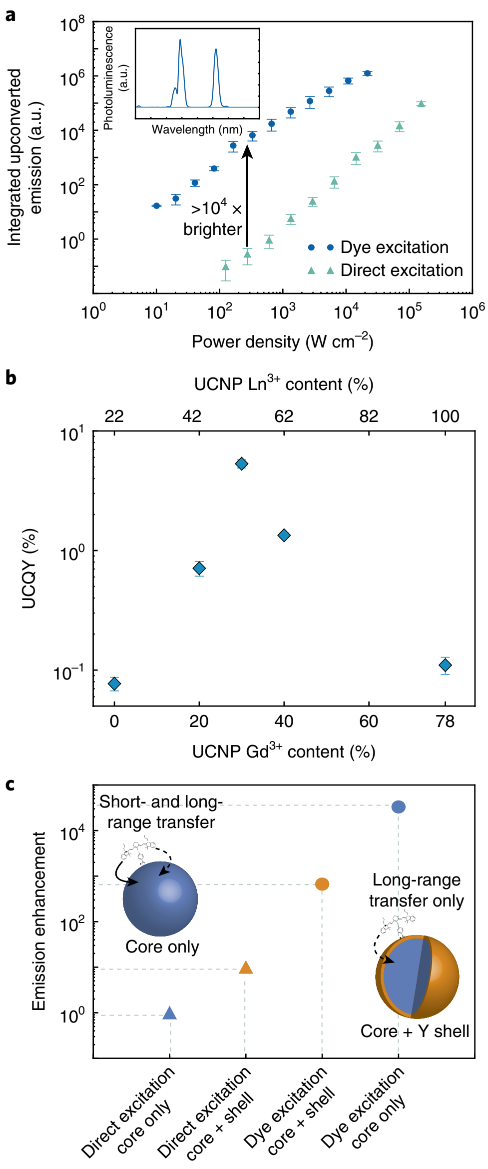

Fig. 4 | Upconverted performance improvements by enhancing the dye triplet population and coupling pathways. **a**, Excitation power dependence of upconverted emission from $NaY_{0.48}Gd_{0.3}Yb_{0.2}Er_{0.02}F_4$ IR806–UCNP under excitation of the dye (dark blue, 808 nm excitation) or UCNP (light blue, 980 nm excitation). Error bars represent one standard deviation from the mean. Inset, Representative emission spectra for dye or direct excitation. **b**, QYs for $NaY_{0.78-x}Gd_xYb_{0.2}Er_{0.02}F_4$ IR806-UCNPs. The amount of Gd^{3+} substituted for Y^{3+} is noted on the bottom x axis, while the total Ln^{3+} content (that is, the sum of Gd^{3+}, Yb^{3+} and Er^{3+} contents) is given on the top axis. UCQYs were measured with 5 W cm^{-2}, 800 nm excitation. Error bars indicate standard deviation, which may be smaller than the symbol. **c**, Emission enhancement from directly excited 30% Gd^{3+} cores (blue triangle), directly excited 20% Gd^{3+} cores coated with a 1.2 nm $NaYF_4$ shell (orange triangle), the same core–shell UCNPs but dye-sensitized (orange circle), and dye-sensitized 30% Gd^{3+} cores (blue circle).

photocleaved in ambient atmosphere (Supplementary Fig. 11), as has been observed with other cyanine dyes[36], and we find that this photocleavage is enhanced when bound to the UCNP (Supplementary Fig. 12). Dispersions of IR806–UCNP conjugates prepared under N_2 are stable (Fig. 3d), showing no measurable photodegradation after continuous excitation for 30 min. Encapsulation of IR806–UCNP films in polymer under N_2 (Supplementary Methods) leads to an order of magnitude increase in photostability over ambient films, and these polymers may be further optimized akin to methods used for preparing stable perovskite-based photovoltaic devices[37]. These results provide further evidence that the heavy lanthanide ions on the UCNP surface enhance ISC rates and subsequent triplet populations within the dye, and highlight that isolation from O_2 and H_2O through encapsulation[38] is paramount to achieving long-term stability of dye-sensitized UCNPs.

Upconversion enhancement factor and quantum efficiency

We measured the upconverted emission of the 30% Gd^{3+} nanoparticles under a wide range of excitation densities, comparing excitation through the dye antennas with direct lanthanide excitation. Even at low powers (~1.8 W cm^{-2}), upconverted emission is noticeable by eye when exciting the dye antennas, but not via direct UCNP excitation (Supplementary Fig. 13). Quantitatively, dye-sensitized upconverted emission is enhanced ~33,000-fold over bare UCNPs (at 200 W cm^{-2} excitation density; Fig. 4a and Supplementary Figs. 14 and 15), and if we take into account the broad molecular absorption band of IR806 compared with the UCNP atomic transitions (Fig. 2c), the dye–UCNP system here could be ~100,000-fold brighter than the bare UCNPs under broadband excitation[1]. Importantly, this signal enhancement originates from the large absorption cross-section of the dye relative to lanthanides, as well as significant improvements in energy transfer and upconversion efficiencies achieved by enriching molecular triplet states. This lowers the excitation intensity required to saturate the lanthanide intermediate energy states, promoting more efficient upconversion at lower powers. Maximizing this effect by capitalizing on both singlet and triplet energy transfer pathways is key to achieving optimal efficiencies while reducing input power.

To further investigate the role of Ln^{3+} content for enhancing IR806 triplets and energy transfer, we synthesized additional UCNPs with varying Gd^{3+} content and determined their IR806–UCNP QYs (Fig. 4b). With constant 20% Yb^{3+} and 2% Er^{3+}, the UCQY shows a strong dependence on Gd^{3+} content, with a maximum UCQY of 5.3 ± 0.4% using 30% Gd^{3+} ($\lambda_{ex} = 808$ nm at 5 W cm^{-2}). This represents an ~100-fold increase over the same UCNPs without IR806 and is comparable to bulk upconverting materials[39] (Supplementary Fig. 16), and additionally provides clear evidence that ISC within the dye ligands plays an integral role in UCNP sensitization. Above ~30% Gd^{3+} content, IR806-functionalized UCNPs show decreasing UCQYs, and 78% Gd^{3+} content UCNP QYs are similar to those of 0% Gd^{3+} UCNPs (Fig. 4b). This suggests that Gd^{3+}, although optically inert at 980 nm, has additional optical properties that may interact with Yb^{3+} or Er^{3+}. One confounding factor may be the Gd^{3+} UV transitions, which have been shown to facilitate energy migration in UCNPs at higher fluences[31] and could interact with Er^{3+} UV manifolds or lead to faster energy migration to surface traps.

Because of the nonlinear nature of the upconversion process, its efficiency increases with the excitation rate. The dyes, with absorption cross-sections ~1,000 times larger than those of UCNPs[1], function as molecular light concentrators, funnelling orders of magnitude more excitation energy into the UCNP. This lowers the excitation intensity required to saturate the lanthanide intermediate energy states, promoting more efficient upconversion at lower powers. Maximizing this effect by capitalizing on both singlet and triplet energy transfer pathways is key to achieving optimal efficiencies while reducing input power, which eliminates a major impediment of using UCNPs for reducing phototoxicity in bioimaging or boosting solar cell efficiency[2,3].

Energy-transfer distance dependence

Finally, we gained further insight into energy transfer and enhancement mechanisms by comparing dye sensitization effects on core-only and core–shell UCNPs with the triplet enhancer Gd^{3+} (Fig. 4c). It is well known that a thin inert shell enhances upconversion by passivating surface-related energy loss pathways[12,40,41]. Dye sensitization of these core–shell UCNPs produces additional upconversion enhancements that, while significant, are roughly one to two orders of magnitude less than what is achieved by dye-sensitizing the core-only 30% Gd^{3+} UCNPs. This discrepancy occurs despite the shell thickness (1.2 nm) being smaller than the dye–Yb^{3+} FRET distance of ~1.5 nm (ref. [15]). Similar dye-sensitized enhancements are seen for other shell thicknesses, including $NaGdF_4$ shells (Supplementary Fig. 15). These results emphasize two key points. First, while longer-range resonant energy transfer from the singlet to the UCNP contributes to enhanced upconversion, other short-range (for example, Dexter-like) pathways clearly contribute. Second, when adding a passivating shell, there is an inherent trade-off between reducing surface-related losses and eliminating short-range energy transfer processes. These conclusions highlight a potential avenue for further optimized systems based on more complex heterostructures and computational approaches[7,15–17,42].

Conclusions

We have demonstrated that triplet states in dye antennas critically affect the brightness and stability of dye–UCNP systems, revealing a clear strategy that overcomes the limitations of previous materials. We find that ISC within the dye is enhanced by spin–orbit coupling to lanthanide ions near the surface of the UCNPs and further that this enriched triplet population is responsible for a significant amount of the energy transferred into the UCNP. Designing dyes whose excited-state wavefunctions sit closer to the nanocrystal surface may further boost energy transfer by enhancing sub-nanometre processes such as spin–orbit coupling and Dexter electron transfer. Also, tuning the UCNP composition to higher active lanthanide content or heavier lanthanides such as Lu^{3+} may lead to further upconversion enhancements. Leveraging this nuanced mechanistic understanding results in superior dye–UCNP performance, which is now poised to drive improvements in solar energy conversion, infrared detection and biological applications.

Data availability. The data that support the plots and other findings within this paper are available from the corresponding author upon reasonable request.

Received: 13 June 2017; Accepted: 14 March 2018;

References

1. Zou, W., Visser, C., Maduro, J. A., Pshenichnikov, M. S. & Hummelen, J. C. Broadband dye-sensitized upconversion of near-infrared light. *Nat. Photon.* **6**, 560–564 (2012).
2. Zhou, B., Shi, B., Jin, D. & Liu, X. Controlling upconversion nanocrystals for emerging applications. *Nat. Nanotech.* **10**, 924–936 (2015).
3. Briggs, J. A., Atre, A. C. & Dionne, J. A. Narrow-bandwidth solar upconversion: case studies of existing systems and generalized fundamental limits. *J. Appl. Phys.* **113**, 124509 (2013).
4. Park, Y. Il, Lee, K. T., Suh, Y. D. & Hyeon, T. Upconverting nanoparticles: a versatile platform for wide-field two-photon microscopy and multi-modal in vivo imaging. *Chem. Soc. Rev.* **44**, 1302–1317 (2014).
5. Liu, Y. et al. Amplified stimulated emission in upconversion nanoparticles for super-resolution nanoscopy. *Nature* **543**, 229–233 (2017).
6. Wang, C., Li, X. & Zhang, F. Bioapplications and biotechnologies of upconversion nanoparticle-based nanosensors. *Analyst.* **141**, 3601–3620 (2016).
7. Wu, X. et al. Dye-sensitized core/active shell upconversion nanoparticles for optogenetics and bioimaging applications. *ACS Nano* **10**, 1060–1066 (2016).
8. Hososhima, S. et al. Near-infrared (NIR) up-conversion optogenetics. *Sci. Rep.* **5**, 16533 (2015).
9. Schmidt, T. W. & Castellano, F. N. Photochemical conversion: the primacy of kinetics. *J. Phys. Chem. Lett.* **5**, 4062–4072 (2014).
10. Schulze, T. F. & Schmidt, T. W. Photochemical upconversion: present status and prospects for its application to solar energy conversion. *Energy Environ. Sci.* **8**, 103–125 (2015).
11. Olivier, J. H. et al. Near-infrared-to-visible photon upconversion enabled by conjugated porphyrinic sensitizers under low-power noncoherent illumination. *J. Phys. Chem. A* **119**, 5642–5649 (2015).
12. Gargas, D. J. et al. Engineering bright sub-10-nm upconverting nanocrystals for single-molecule imaging. *Nat. Nanotech.* **9**, 300–305 (2014).
13. Wu, S. et al. Non-blinking and photostable upconverted luminescence from single lanthanide-doped nanocrystals. *Proc. Natl Acad. Sci. USA* **106**, 10917–10921 (2009).
14. Park, Y. Il et al. Nonblinking and nonbleaching upconverting nanoparticles as an optical imaging nanoprobe and T_1 magnetic resonance imaging contrast agent. *Adv. Mater.* **21**, 4467–4471 (2009).
15. Chen, G. et al. Energy-cascaded upconversion in an organic dye-sensitized core/shell fluoride nanocrystal. *Nano Lett.* **15**, 7400–7407 (2015).
16. Shao, W. et al. Tunable narrow band emissions from dye-sensitized core/shell/shell nanocrystals in the second near-infrared biological window. *J. Am. Chem. Soc.* **138**, 16191–16195 (2016).
17. Chen, G. et al. Efficient broadband upconversion of near-infrared light in dye-sensitized core/shell nanocrystals. *Adv. Opt. Mater.* **4**, 1760–1766 (2016).
18. Lee, J. et al. Ultra-wideband multi-dye-sensitized upconverting nanoparticles for information security application. *Adv. Mater.* **29**, 1603169 (2017).
19. Du, C., Wang, H., Yang, F. & Hammel, P. C. Systematic variation of spin–orbit coupling with *d*-orbital filling: large inverse spin Hall effect in 3*d* transition metals. *Phys. Rev. B* **90**, 140407(R) (2014).
20. Klink, S. I., Keizer, H. & van Veggel, F. C. J. M. Transition metal complexes as photosensitizers for near-infrared lanthanide luminescence. *Angew. Chem. Int. Ed.* **39**, 4319–4321 (2000).
21. Beeby, A., Faulkner, S., Parker, D. & Williams, J. A. G. Sensitised luminescence from phenanthridine appended lanthanide complexes: analysis of triplet mediated energy transfer processes in terbium, europium and neodymium complexes. *J. Chem. Soc. Perkin Trans.* **2**, 1268–1273 (2001).
22. Faulkner, S., Natrajan, L. S., Perry, W. S. & Sykes, D. Sensitised luminescence in lanthanide containing arrays and *d–f* hybrids. *Dalton Trans.* 3890–3899 (2009).
23. Klink, S. I. et al. A systematic study of the photophysical processes in polydentate triphenylene-functionalized Eu^{3+}. *J. Phys. Chem. A* **104**, 5457–5468 (2000).
24. Bunzli, J. G. & Piguet, C. Taking advantage of luminescent lanthanide ions. *Chem. Soc. Rev.* **34**, 1048–1077 (2005).
25. Thompson, N. J. et al. Energy harvesting of non-emissive triplet excitons in tetracene by emissive PbS nanocrystals. *Nat. Mater.* **13**, 1039–1043 (2014).
26. Cedric, M., Garakyaraghi, S., Razgoniaeva, N., Zamkov, M. & Castellano, F. N. Direct observation of triplet energy transfer from semiconductor nanocrystals. *Science* **351**, 369–372 (2016).
27. Tabachnyk, M. et al. Resonant energy transfer of triplet excitons from pentacene to PbSe nanocrystals. *Nat. Mater.* **13**, 1033–1038 (2014).
28. Agbo, P., Xu, T., Sturzbecher-Hoehne, M. & Abergel, R. J. Enhanced ultraviolet photon capture in ligand-sensitized nanocrystals. *ACS Photon.* **3**, 547–552 (2016).
29. Huang, Z. et al. Hybrid molecule-nanocrystal photon upconversion across the visible and near-infrared. *Nano. Lett.* **15**, 5552–5557 (2015).
30. Piland, G. B., Huang, Z., Lee Tang, M. & Bardeen, C. J. Dynamics of energy transfer from CdSe nanocrystals to triplet states of anthracene ligand molecules. *J. Phys. Chem. C* **120**, 5883–5889 (2016).
31. Wang, F. et al. Tuning upconversion through energy migration in core–shell nanoparticles. *Nat. Mater.* **10**, 968–973 (2011).
32. Marling, J. B., Gregg, D. W. & Wood, L. Chemical quenching of the triplet state in flashlamp-excited liquid organic lasers. *Appl. Phys. Lett.* **17**, 527–530 (1970).
33. Pappalardo, R., Samelson, H. & Lempicki, A. Long pulse laser emission from rhodamine 6G using cyclooctatetraene. *Appl. Phys. Lett.* **16**, 267–269 (1970).
34. Schols, S., Kadashchuk, A., Heremans, P., Helfer, A. & Scherf, U. Triplet excitation scavenging in films of conjugated polymers. *ChemPhysChem* **10**, 1071–1076 (2009).
35. Schaap, A. P. *Singlet Molecular Oxygen* (Dowden, Hutchinson, & Ross: Stroudsburg, PA, 1976).
36. Gorka, A. P., Nani, R. R., Zhu, J., Mackem, S. & Schnermann, M. J. A near-IR uncaging strategy based on cyanine photochemistry. *J. Am. Chem. Soc.* **136**, 14153–14159 (2014).
37. Han, Y. et al. Degradation observations of encapsulated planar $CH_3NH_3PbI_3$ perovskite solar cells at high temperatures and humidity. *J. Mater. Chem. A* **3**, 8139–8147 (2015).
38. Ow, H. et al. Bright and stable core–shell fluorescent silica nanoparticles. *Nano Lett.* **5**, 113–117 (2005).
39. Pokhrel, M., Kumar, G. A. & Sardar, D. K. Highly efficient NIR to NIR and VIS upconversion in Er^{3+} and Yb^{3+} doped in M_2O_2S (M = Gd, La, Y). *J. Mater. Chem. A* **1**, 11595–11606 (2013).

40. Fischer, S., Bronstein, N. D., Swabeck, J. K., Chan, E. M. & Alivisatos, A. P. Precise tuning of surface quenching for luminescence enhancement in core–shell lanthanide-doped nanocrystals. *Nano Lett.* **16**, 7241–7247 (2016).
41. Johnson, N. J. J. et al. Direct evidence for coupled surface and concentration quenching dynamics in lanthanide-doped nanocrystals. *J. Am. Chem. Soc.* **139**, 3275–3282 (2017).
42. Chan, E. M., Levy, E. S. & Cohen, B. E. Rationally designed energy transfer in upconverting nanoparticles. *Adv. Mater.* **27**, 5753–5761 (2015).

Acknowledgements

The authors thank S. Fischer, K. Raymond and K. Yao for helpful discussions, and T. Chen for her invaluable experimental assistance. This work was supported by the National Science Foundation SAGE IGERT fellowship (to D.J.G.) and the Chinese Scholarship Council fellowship (B.T.). Portions of this research were supported by the Global Research Laboratory (GRL) Program through the National Research Foundation of Korea (NRF) funded by the Ministry of Science and ICT (no. 2016911815). This work was performed at the Molecular Foundry and was supported by the Office of Science, Office of Basic Energy Sciences, of the US Department of Energy (contract no. DE-AC02-05CH11231). The computational work performed here was supported by the Director, Office of Science, Chemical Sciences, Geosciences and Biosciences Division of the US Department of Energy, under contract no. DEAC02-05CH1123.

Author contributions

The scientific concepts, ideas and experimental designs were the result of interactions and discussions between D.J.G., P.J.S., B.E.C., N.J.B., E.M.C. and Y.D.S. D.J.G., E.M.C., N.A.T., C.A.T. and B.T. synthesized the nanoparticles. D.J.G., N.J.B. and E.S.B. conducted the spectroscopic measurements. D.J.G. and E.M.C. conducted the QY measurements. S.M.H. and J.B.N. performed the theoretical modelling. B.S. and S.A. conducted the electron microscopy. D.J.G., N.J.B., E.M.C., B.E.C. and P.J.S. wrote the paper, in coordination with all the authors.

Competing interests

The authors declare no competing interests.

Additional information

Supplementary information is available for this paper at https://doi.org/10.1038/s41566-018-0156-x.

Reprints and permissions information is available at www.nature.com/reprints.

Correspondence and requests for materials should be addressed to E.M.C. or B.E.C. or P.J.S.

Publisher's note: Springer Nature remains neutral with regard to jurisdictional claims in published maps and institutional affiliations.